Gene Reports 37 (2024) 102063

Contents lists available at ScienceDirect

Gene Reports

journal homepage: www.elsevier.com/locate/genrep

Intra-segmental recombinations between avian and mammalian VP4 genotypes in *Rotavirus alphagastroenteritidis*

Yoshiyuki Suzuki *, Masaya Yaeshiro, Daiki Uehara

Graduate School of Science, Nagoya City University, 1 Yamanohata, Nagoya-shi, Aichi-ken 467-8501, Japan

ARTICLE INFO

Edited by Dominic Voon

Keywords:
Genomic segment
Genotype
Phylogenetic tree
Reassortment
Recombination
Rotavirus

ABSTRACT

Rotavirus alphagastroenteritidis (RVA), a pathogen causing acute gastroenteritis in young birds and mammals, possesses a genome of 11 segmented double-stranded RNAs, each of which is classified into genotypes. RVA has been divided into the avian and mammalian clusters as well as the basal group. Although the avian and mammalian clusters were considered to have evolved independently, genomic segment encoding viral protein 4 (VP4) of pheasant strain with genotype P[37] appeared to be transferred from mammalian cluster strain through reassortment. Here prototype sequences for all genotypes P[1]-P[58] of VP4 segment except for P[53] and P[54] retrieved from the International Nucleotide Sequence Database were analyzed to examine the possibility that P[37] was a product of intra-segmental recombinations between avian and mammalian cluster strains. In the sliding window analysis, different regions of P[37] appeared to have different relative similarities to avian and mammalian cluster strains. Using recombination detection programs, two regions of P[37] were identified to be derived from mammalian cluster strains and integrated into the background of avian cluster strain. These results were confirmed by phylogenetic analyses. Thus, even when genomic segments are not entirely compatible between strains, only compatible parts may be transferred through intra-segmental recombinations in RVA.

1. Introduction

Rotavirus alphagastroenteritidis (RVA), a species belonging to the family *Sedoreoviridae*, order *Reovirales*, is a pathogen causing acute gastroenteritis in young birds and mammals (Bishop et al., 1973). The RVA genome consists of 11 segments of double-stranded RNAs (dsRNAs) with a total length of ~18.5 kbp (Mitchell and Both, 1990). Each genomic segment encodes either viral protein 1 (VP1), VP2, VP3, VP4, VP6, VP7, non-structural protein 1 (NSP1), NSP2, NSP3, NSP4, or NSP5/NSP6.

The RVA virion is a non-enveloped, icosahedral, triple-layered particle (TLP) with a diameter of ~100 nm (Jayaram et al., 2004). Genomic dsRNAs attached to VP1 RNA-dependent RNA polymerase and VP3 capping enzyme are enclosed in the innermost layer of VP2 to construct the core, which is surrounded by the intermediate layer of VP6 to form the double-layered particle (DLP). The outermost layer of TLP is composed of VP7 surface glycoprotein and VP4 spike protein, which are targets of adaptive immunity containing neutralization epitopes.

The RVA infection is initiated with binding of the spike composed of VP4 trimer to cellular receptors (Xu et al., 2020; Falkenhagen et al., 2021). VP4 is cleaved into VP8* containing α segment and lectin domain and VP5* containing β-barrel and C-terminal domains. Lectin domain constitutes the globular head of VP4, and is responsible for receptor binding. β-barrel domain forms the body and stalk of VP4, containing hydrophobic loops, which are inserted into cellular membrane. C-terminal domain together with α segment constitutes the foot of VP4, which interacts with VP6 and VP7 to be anchored to the outermost layer of TLP (Settembre et al., 2011; Valusenko-Mehrkens et al., 2023).

The RVA replication occurs in the cytoplasm, where NSP1 antagonizes interferon expression to suppress innate immunity (Arnold, 2016). NSP2 forms viroplasms together with NSP5/6, and binds to the RVA positive-sense RNAs (+RNAs) to mediate conformational changes and facilitate interactions among them (Borodavka et al., 2017). NSP3 binds to 3′ terminal regions of the RVA +RNAs to promote circularization and enhance translation. NSP4, an enterotoxin, is expressed on rough endoplasmic reticulum as the receptor for DLP.

The RVA classification system has been developed based on genotyping of each genomic segment (Matthijnssens et al., 2008). So far, VP7, VP4, VP6, VP1, VP2, VP3, NSP1, NSP2, NSP3, NSP4, and NSP5/6 segments have been classified into 42 G, 58 P, 32 I, 28 R, 24 C, 24 M, 39 A, 28 N, 28 T, 32 E, and 28 H genotypes, respectively (Rotavirus

* Corresponding author.
E-mail address: yossuzuk@nsc.nagoya-cu.ac.jp (Y. Suzuki).

https://doi.org/10.1016/j.genrep.2024.102063
Received 24 July 2024; Received in revised form 19 September 2024; Accepted 12 October 2024
Available online 17 October 2024

List of abbreviations

DLP	double-layered particle
dsRNA	double-stranded RNA
F	equilibrium frequencies of amino acids as estimated from data
Γ	gamma-distributed rate heterogeneity among sites
GTR	general time reversible model
I	invariable sites
INSD	International Nucleotide Sequence Database
LG	Le-Gascuel model
ML	maximum likelihood
NJ	neighbor-joining
NSP	non-structural protein
P	probability
RCWG	Rotavirus Classification Working Group
+RNA	positive-sense RNA
RVA	*Rotavirus alphagastroenteritidis*
TLP	triple-layered particle
VP	viral protein

Classification Working Group: RCWG, 2021). Each RVA strain is characterized with a genotype constellation designated as Gx-P[x]-Ix-Rx-Cx-Mx-Ax-Nx-Tx-Ex-Hx, where x's denote genotype numbers (Matthijnssens et al., 2011).

Traditionally, RVA had been divided into two phylogenetically distinct clusters consisting of strains infecting birds (avian cluster) and mammals (mammalian cluster) (Ito et al., 2001; Trojnar et al., 2009). Recently, however, several strains that apparently have diverged earlier than the split of the avian and mammalian clusters were identified in both birds (e.g., common gulls) (Fujii et al., 2022) and mammals (e.g., common shrews) (Falkenhagen et al., 2022; Johne et al., 2023), constituting the basal group of RVA.

Due to the segmented nature of the genome, reassortment is a major evolutionary mechanism in RVA (Nakagomi and Nakagomi, 2002). However, since the avian and mammalian clusters were always separated in phylogenetic trees for all genomic segments, these clusters were considered to have evolved independently without reassortment, until unusual strains 10V0112H5 and 216/2015 with genotype constellation G23-P[37]-I4-R4-C4-M4-A16-N10-T4-E4-H4 were isolated from pheasant (Trojnar et al., 2013; Gal et al., 2016). In phylogenetic analyses, all genomic segments except for VP4 segment supported the classification of pheasant strains into the avian cluster, whereas VP4 segment supported the classification into the mammalian cluster. According to these results, it was postulated that pheasant strains were generated through reassortment between avian and mammalian cluster strains.

Reassortment potential between avian and mammalian cluster strains has also been investigated experimentally. Co-infection of cell-lines with turkey strain Ty-1 (VP4 genotype P[38]) and simian strain RRV (P[3]) yielded a mono-reassortant containing VP4 segment of RRV in the Ty-1 backbone (Kool et al., 1992). Using the reverse genetics system for simian strain SA11 (P[2]), mono-reassortants containing VP4 segment of pheasant strain 10V0112H5 (P[37]) as well as VP3 or VP4 segment of chicken strain 02V0002G3 (P[30]) in the SA11 backbone could be rescued (Johne et al., 2016; Falkenhagen et al., 2019; Patzina-Mehling et al., 2020). Notably, however, these reassortants proliferated less efficiently than SA11. In addition, attempts to generate a mono-reassortant containing VP4 segment of turkey strain 03V0002E10 (P[35]) in the SA11 backbone failed. These observations suggested that VP4 segment of avian cluster strains was not entirely compatible with mammalian cluster strains and *vice versa*, and that VP4 segment of pheasant strain was not distinguishable from those of avian cluster strains in terms of compatibility to mammalian cluster strains. It was therefore questionable whether VP4 segment of pheasant strain was really derived from mammalian cluster strain through reassortment.

Recently accumulating evidence suggests that not only reassortment but also intra-segmental, homologous recombination may be a significant evolutionary mechanism in the order *Reovirales*, including RVA (Suzuki et al., 1998; Hoxie and Dennehy, 2020), *R. tritogastroenteritidis* (Oki et al., 2022), *Orbivirus alphaequi* (Ngoveni et al., 2019), *O. caerulinguae* (He et al., 2010), *O. ruminantium* (Anthony et al., 2009), *Cypovirus altineae* (Zhang et al., 2020), *Fijivirus alporyzae* (Yin et al., 2013), *F. boryzae* (Li et al., 2013), and *Orthoreovirus mammalis* (Fukase et al., 2022). The purpose of the present study was to examine the possibility that genotype P[37] VP4 segment of pheasant strain was a product of intra-segmental recombinations between avian and mammalian cluster strains in RVA.

2. Materials and methods

2.1. Sequence data

Prototype sequences for all genotypes P[1]-P[58] of VP4 segment in RVA were retrieved from the International Nucleotide Sequence Database (INSD), except for P[53] and P[54], which were missing (Supplementary Table S1). For each genotype, the nucleotide sequence region encoding VP4 was extracted and translated into the amino acid sequence. Multiple alignments were made for the total of 56 nucleotide sequences as well as amino acid sequences by MAFFT (version 7.427) (Katoh et al., 2002).

2.2. Data analysis

Assuming that P[37] was generated through intra-segmental recombinations between avian and mammalian cluster strains, different parts of P[37] may have different relative similarities to these strains. Thus, local similarities of P[37] to avian and mammalian cluster strains were examined by the sliding window analysis applying a self-made computer program to multiple alignment of nucleotide sequences with the window and step sizes set to be 100 and 10, respectively. In each step, average nucleotide identity between P[37] and avian cluster strains as well as mammalian cluster strains within the window was computed eliminating the sites with gaps or ambiguous nucleotides. Multiple alignment of nucleotide sequences was also analyzed for detecting signatures of intra-segmental recombinations in P[37] by using recombination detection programs including RDP, GENECONV, BootScan, MaxChi, Chimera, SiScan, and 3Seq implemented in RDP4 (version 4.101) (Martin et al., 2015).

Phylogenetic analyses were conducted on nucleotide and amino acid sequences for various parts of VP4 by MEGA (version 10.1.7) (Kumar et al., 2018). After eliminating the sites with gaps or ambiguous characters, the best fit model of nucleotide or amino acid substitutions was selected based on the corrected Akaike information criterion (Table 1). Phylogenetic trees were constructed using the maximum likelihood (ML) method based on the best fit model and the neighbor-joining (NJ) method based on the p distance, which was reported to produce more reliable topologies than the ML method (Nei and Kumar, 2000; Yoshida and Nei, 2016). Reliabilities of interior branches were assessed by the bootstrap method with 1000 re-samplings. Phylogenetic trees were visualized by FigTree (version 1.4.4) (Rambaut, 2018). P[55] was assumed to have diverged first among all genotypes of VP4, as reported in Falkenhagen et al. (2022).

3. Results

3.1. Local similarities of P[37] to avian and mammalian cluster strains

When ML and NJ trees were constructed using nucleotide and amino acid sequences for the whole region of VP4, the sequences could be

Table 1
Phylogenetic position of P[37] in ML and NJ trees constructed using nucleotide and amino acid sequences.

Region	Nucleotide sequence				Amino acid sequence			
	Sites[a]	Model[b]	ML tree[c]	NJ tree[c]	Sites[a]	Model[b]	ML tree[c]	NJ tree[c]
Whole	1873	GTR + Γ + I	Mammalian (0.96)[S1]	**Mammalian (0.99)**[S2]	622	LG + Γ + I + F	Mammalian (0.91)[S3]	Mammalian (0.90)[S4]
M1	539	GTR + Γ + I	Mammalian (0.89)[S6]	Mammalian (0.92)[S7]	189	LG + Γ + I + F	Mammalian (0.87)[S8]	**Mammalian (0.96)**[S9]
A1	800	GTR + Γ + I	Mammalian (0.40)[S10]	Mammalian (0.48)[S11]	261	LG + Γ + F	**Avian (0.85)**[S12]	Avian (0.82)[S13]
M2	197	GTR + Γ + I	Avian (0.08)[S18]	Avian (0.07)[S19]	58	LG + Γ	Basal (0.05)[S20]	**Mammalian (0.12)**[S21]
A2	337	GTR + Γ + I	**Avian (0.18)**[S22]	Basal (0.05)[S23]	112	LG + Γ + I	Avian (0.14)[S24]	Avian (0.14)[S25]
A12	1137	GTR + Γ + I	Mammalian (0.31)[S14]	Mammalian (0.43)[S15]	373	LG + Γ + F	Avian (0.78)[S16]	**Avian (0.81)**[S17]

[a] Number of sites retained in multiple alignment after eliminating the sites with gaps or ambiguous characters.
[b] The best fit model of nucleotide or amino acid substitutions; GTR: general time reversible model, Γ: gamma-distributed rate heterogeneity among sites, I: invariable sites, LG: Le-Gascuel model (Le and Gascuel, 2008), and F: equilibrium frequencies of amino acids as estimated from data.
[c] Phylogenetic position of P[37]; Mammalian: mammalian cluster, Avian: avian cluster, and Basal: basal group. Bootstrap probability supporting the phylogenetic position of P[37] is indicated in parentheses. For each region, the result with the highest bootstrap probability is bold-faced and underlined. Superscripts S1-S4 and S6-S25 indicate Supplementary Figs. S1–S4 and S6–S25, respectively.

largely divided into the avian cluster, mammalian cluster, and basal group (Supplementary Figs. S1–S4). The avian cluster consisted of P[17], P[30], P[31], P[35], P[38], and P[56], and the basal group consisted of P[39], P[44], P[55], and P[58]. The mammalian cluster consisted of the remaining sequences except for P[11], which was included in the avian cluster and basal group using nucleotide and amino acid sequences, respectively. In all trees, P[37] was located in the mammalian cluster, which was consistent with the hypothesis that P[37] was derived from mammalian cluster strain through reassortment (Trojnar et al., 2013; Gal et al., 2016).

Local nucleotide identities of P[37] with avian and mammalian cluster strains as examined by the sliding window analysis were largely comparable (Fig. 1). However, it was evident that positions ~200- ~700 of P[37] had a greater similarity to mammalian cluster strains than avian cluster strains. Reportedly, at the cleavage site of VP8* and VP5* (positions 712–723; numberings according to pheasant strain 10V0112H5 with the INSD accession number JX204814), P[37] was more closely related to mammalian cluster strains than avian cluster strains (Fujii et al., 2022). In the present study, it was observed that P[37] contained a deletion of six nucleotide sites between positions 728 and 729, which was specific to avian cluster strains (Supplementary Fig. S5). These observations suggested that there may be a boundary located between positions 723 and 728, whose upstream and downstream regions were derived from mammalian and avian cluster strains, respectively.

3.2. Detection of intra-segmental recombinations in P[37]

By using recombination detection programs, two regions were identified to be derived from mammalian cluster strains and integrated into the background of avian cluster strain in P[37] (Fig. 1). The first

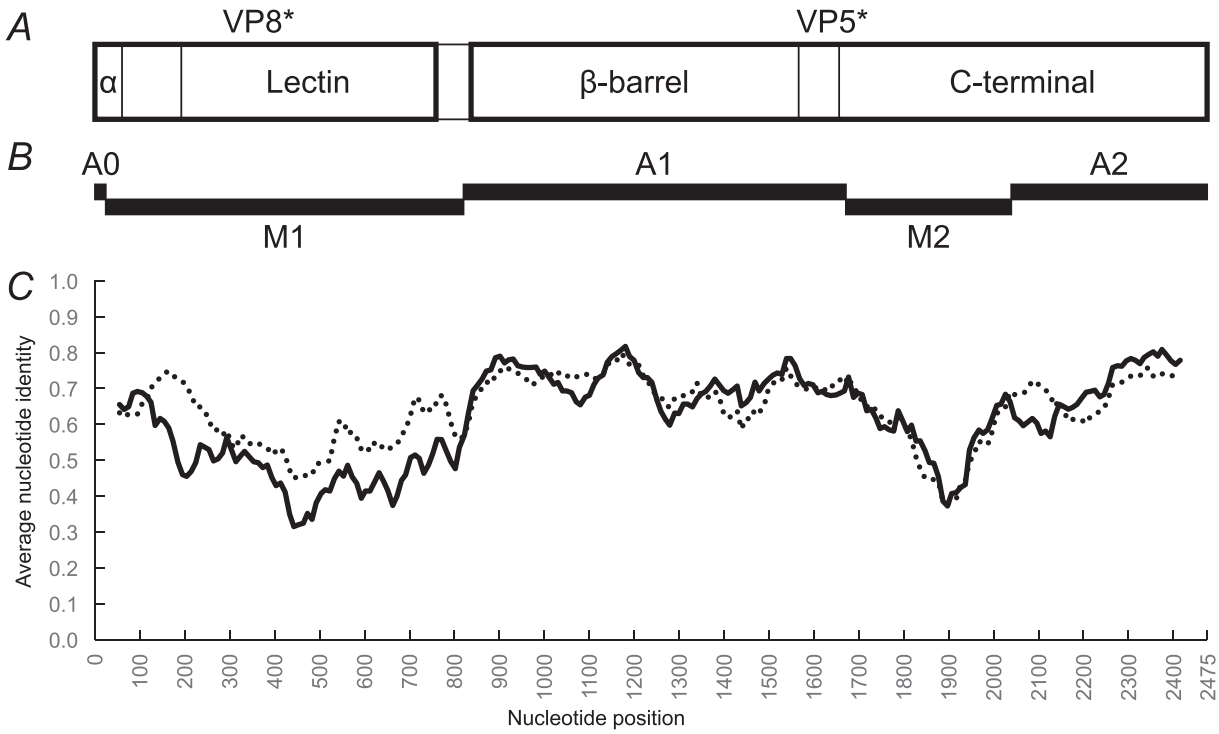

Fig. 1. *A*. VP4 is cleaved into VP8* containing α segment and lectin domain and VP5* containing β-barrel and C-terminal domains. *B*. Division of the whole region of P[37] VP4 into A0, A1, and A2 regions possibly derived from avian cluster strain and M1 and M2 regions possibly derived from mammalian cluster strains. *C*. Local nucleotide identities of P[37] with avian (solid line) and mammalian (dotted line) cluster strains obtained by the sliding window analysis with the window and step sizes set to be 100 and 10, respectively. For each window spanning positions $(1 + 10x)$-$(100 + 10x)$ $(0 \leq x \leq 237)$, average nucleotide identities are plotted at position $50 + 10x$.

region (positions 25–724), identified by MaxChi ($P = 1.490 \times 10^{-2}$), Chimera ($P = 1.432 \times 10^{-6}$), and SiScan ($P = 8.789 \times 10^{-7}$), was inferred to be derived from mammalian cluster strain with P[27]. Notably, the 3′ end of this region (position 724) matched the location of the aforementioned boundary (between positions 723 and 728) whose upstream and downstream regions were predicted to be derived from mammalian and avian cluster strains, respectively (Supplementary Fig. S5). The second region (positions 1537–1859), identified by MaxChi ($P = 6.083 \times 10^{-3}$) and SiScan ($P = 7.980 \times 10^{-3}$), was inferred to be derived from mammalian cluster strain with P[47]. Both regions were inferred to be integrated into the background of avian cluster strain with P[30]. According to these results, the whole region of VP4 was divided into possibly avian cluster strain-derived region 0 (A0 region) (positions 1–24), possibly mammalian cluster strain-derived region 1 (M1 region) (positions 25–724), A1 region (positions 725–1536), M2 region (positions 1537–1859), and A2 region (positions 1860–2289). Interestingly, these regions largely corresponded to structural and functional domains of VP4 (fig. 1).

3.3. Phylogenetic position of P[37]

Phylogenetic analyses were conducted for A1, M1, A2, and M2 regions, but not for A0 region, because the number of sites included was small (24 nucleotide and eight amino acid sites) and all sites contained gaps. In addition, A1 and A2 regions were concatenated into A12 region, because both regions were inferred to be derived from P[30] by recombination detection programs, as described above. In ML and NJ trees constructed using nucleotide and amino acid sequences for each region, the sequences could be largely divided into the avian cluster, mammalian cluster, and basal group, although constituent sequences slightly varied. P[37] was always included in the mammalian cluster for M1 region (Supplementary Figs. S6–S9), but phylogenetic position of P[37] was not stable for other regions. That is, P[37] was included in the avian and mammalian clusters for A1 (Supplementary Figs. S10–S13) and A12 regions (Supplementary Figs. S14–S17), in the avian and mammalian clusters as well as the basal group for M2 region (Supplementary Figs. S18–S21), and in the avian cluster and basal group for A2 region (Supplementary Figs. S22–S25). Nevertheless, when bootstrap probabilities supporting the position of P[37] were compared between phylogenetic trees for each region, P[37] was inferred to be included in the avian cluster for A1, A2, and A12 regions and in the mammalian cluster for M1 and M2 regions with the greatest reliability (Table 1). These observations were consistent with the results obtained from sliding window analyses and recombination detection programs, as described above.

4. Discussion

4.1. Occurrences of intra-segmental recombinations for generating P[37]

In the present study, the results obtained from sliding window analyses, recombination detection programs, and phylogenetic analyses collectively indicated that P[37] was generated through intra-segmental recombinations between avian and mammalian cluster strains. Although signatures of intra-segmental recombinations could also be generated as sequencing artifacts (Woods, 2015), this was not likely to be the case because similar sequences of P[37] were obtained by Sanger and random sequencing techniques applied to two pheasant strains that were independently isolated from different countries in different years by different research groups (Trojnar et al., 2013; Gal et al., 2016).

4.2. Regions involved in intra-segmental recombinations in P[37]

Even when genomic segments are not entirely compatible between strains, only compatible parts may be transferred through intra-segmental recombinations in RVA. Recombination breakpoints in P[37] largely corresponded to boundaries between structural and functional domains of VP4, possibly reflecting that domains were a unit of evolution (Gilbert, 1978). Lectin domain interacting with cellular receptors (Xu et al., 2020; Falkenhagen et al., 2021) and a part of C-terminal domain interacting with VP6 and VP7 (Settembre et al., 2011; Valusenko-Mehrkens et al., 2023) appeared to be derived from mammalian cluster strains, whereas the remainder including terminal regions appeared to be derived from avian cluster strain. Notably, RVA has been considered to undergo selective packaging, in which one copy each of 11 genomic segments is packaged into the virion (Borodavka et al., 2017; Fajardo Jr. et al., 2017; Oshima et al., 2022). Upon selective packaging, 11 genomic segments are bundled into a supra-molecular complex through interactions between terminal regions (Li et al., 2010; McDonald and Patton, 2011), which may have caused incompatibility between avian and mammalian cluster strains.

4.3. RVA transmissions between birds and mammals

At least one avian cluster strain and two mammalian cluster strains appeared to be involved in generating P[37], where RVA transmissions between birds and mammals should have occurred at least twice. Indeed, avian cluster strains have been isolated from mammals (Brussow et al., 1992; Mitake et al., 2015; Busi et al., 2017) and mammalian cluster strains have been isolated from birds (Asano et al., 2011). Particularly, large-billed crows (*Corvus macrorhynchos*) are considered to have transmitted RVA to common raccoons (*Procyon lotor*) (Fujii et al., 2024). In addition, basal group strains have been identified in both birds (Fujii et al., 2022) and mammals (Falkenhagen et al., 2022; Johne et al., 2023). These observations suggested that RVA transmissions between birds and mammals may be taking place in nature, although genetic exchanges between avian and mammalian RVAs may be restricted due to incompatibility between genomic segments at the RNA or protein level (Suzuki et al., 2024).

4.4. Possible mechanism of intra-segmental recombinations in RVA

Reportedly, intra-segmental, non-homologous rearrangements occur in RVA through template switching (Desselberger, 1996; Gault et al., 2001; Schnepf et al., 2008; Troupin et al., 2011). Inside the core of the RVA virion, each of 11 genomic segments together with VP1 and VP3 is associated with one of 12 five-fold symmetry vertices, so that one vertex remains available for packaging additional genomic segment (Trask et al., 2012). In addition, the RVA genome occupies only ~50- ~ 60 % of the space and extra >2500 bp can be packaged in the core (Desselberger, 2020). Thus, in RVA, intra-segmental recombinations may occur through template switching when additional genomic segment is packaged into the core, although the frequency may be relatively low (Woods, 2015; Hoxie and Dennehy, 2020).

Supplementary data to this article can be found online at https://doi.org/10.1016/j.genrep.2024.102063.

CRediT authorship contribution statement

Yoshiyuki Suzuki: Writing – original draft, Visualization, Methodology, Formal analysis, Conceptualization. **Masaya Yaeshiro:** Writing – review & editing, Methodology, Formal analysis, Conceptualization. **Daiki Uehara:** Writing – review & editing, Validation, Investigation.

Declaration of competing interest

The authors declare no conflict of interest.

Acknowledgements

The authors thank anonymous reviewers for valuable comments.

This work was supported by JSPS KAKENHI Grant Number JP19K12221 and AMED Grant Number JP23fk0108667 to Y.S.

Data availability

Data will be made available on request.

References

Anthony, S.J., Maan, N., Maan, S., Sutton, G., Attoui, H., Mertens, P.P.C., 2009. Genetic and phylogenetic analysis of the non-structural proteins NS1, NS2 and NS3 of epizootic haemorrhagic disease virus (EHDV). Virus Res. 145, 211–219.

Arnold, M.M., 2016. The rotavirus interferon antagonist NSP1: many targets, many questions. J. Virol. 90, 5212–5215.

Asano, K.M., Gregori, F., Souza, S.P., Rotava, D., Oliveira, R.N., Villarreal, L.Y.B., Richtzenhain, L.J., Brandao, P.E., 2011. Bovine rotavirus in turkeys with enteritis. Avian Dis. 55, 697–700.

Bishop, R.F., Davidson, G.P., Holmes, I.H., Ruck, B.J., 1973. Virus particles in epithelial cells of duodenal mucosa from children with acute non-bacterial gastroenteritis. Lancet 2, 1281–1283.

Borodavka, A., Dykeman, E.C., Schrimpf, W., Lamb, D.C., 2017. Protein-mediated RNA folding governs sequence-specific interactions between rotavirus genome segments. eLife 6, e27453.

Brussow, H., Nakagomi, O., Gerna, G., Eichhorn, W., 1992. Isolation of an avianlike group A rotavirus from a calf with diarrhea. J. Clin. Microbiol. 30, 67–73.

Busi, C., Martella, V., Papetti, A., Sabelli, C., Lelli, D., Alborali, G.L., Gibelli, L., Gelmetti, D., Lavazza, A., Cordioli, P., Boniotti, B.M., 2017. Group A rotavirus associated with encephalitis in red fox. Emerg. Infect. Dis. 23, 1535–1538.

Desselberger, U., 1996. Genome rearrangements of rotaviruses. Adv. Virus Res. 46, 69–95.

Desselberger, U., 2020. What are the limits of the packaging capacity for genomic RNA in the cores of rotaviruses and of other members of the *Reoviridae*? Virus Res. 276, 197822.

Fajardo Jr., T., Sung, P.-Y., Celma, C.C., Roy, P., 2017. Rotavirus genomic RNA complex forms via specific RNA-RNA interactions: disruption of RNA complex inhibits virus infectivity. Viruses 9, 167.

Falkenhagen, A., Patzina-Mehling, C., Rückner, A., Vahlenkamp, T.W., Johne, R., 2019. Generation of simian rotavirus reassortants with diverse VP4 genes using reverse genetics. J. Gen. Virol. 100, 1595–1604.

Falkenhagen, A., Huyzers, M., van Dijk, A.A., Johne, R., 2021. Rescue of infectious rotavirus reassortants by a reverse genetics system is restricted by the receptor-binding region of VP4. Viruses 13, 363.

Falkenhagen, A., Tausch, S.H., Labutin, A., Grutzke, J., Heckel, G., Ulrich, R.G., Johne, R., 2022. Genetic and biological characteristics of species A rotaviruses detected in common shrews suggest a distinct evolutionary trajectory. Virus Evol. 8, veac004.

Fujii, Y., Masatani, T., Nishiyama, S., Okajima, M., Izumi, F., Okazaki, K., Sakoda, Y., Takada, A., Ozawa, M., Sugiyama, M., Ito, N., 2022. Molecular characterisation of a novel avian rotavirus A strain detected from a gull species (*Larus* sp.). J. Gen. Virol. 103 jgv.0.001792.

Fujii, Y., Masatani, T., Nishiyama, S., Takahashi, T., Okajima, M., Izumi, F., Sakoda, Y., Takada, A., Ozawa, M., Sugiyama, M., Ito, N., 2024. Molecular characterization of an avian rotavirus a strain detected from a large-billed crow (*Corvus macrorhynchos*) in Japan. Virology 596, 110114.

Fukase, Y., Minami, F., Masuda, T., Oi, T., Takemae, H., Ishida, H., Murakami, H., Aihara, N., Shiga, T., Kamiie, J., Furuya, T., Mizutani, T., Oba, M., Nagai, M., 2022. Genetic diversity, reassortment, and recombination of mammalian orthoreoviruses from Japanese porcine fecal samples. Arch. Virol. 167, 2643–2652.

Gal, J., Marton, S., Ihasz, K., Papp, H., Jakab, F., Malik, Y.S., Banyai, K., Farkas, S.L., 2016. Complete genome sequence of a genotype G23P[37] pheasant rotavirus strain identified in Hungary. Genome Announc. 4 e00119-16.

Gault, E., Schnepf, N., Poncet, D., Servant, A., Teran, S., Garbarg-Chenon, A., 2001. A Human Rotavirus With Rearranged Genes 7 and 11 Encodes a Modified NSP3 Protein and Suggests an Additional Mechanism for Gene Rearrangement, 75, pp. 7305–7314.

Gilbert, W., 1978. Why genes in pieces? Nature 271, 501.

He, C.-Q., Ding, N.-Z., He, M., Li, S.-N., Wang, X.-M., He, H.-B., Liu, X.-F., Guo, H.-S., 2010. Intragenic recombination as a mechanism of genetic diversity in bluetongue virus. J. Virol. 64, 11487–11495.

Hoxie, I., Dennehy, J.J., 2020. Intragenic recombination influences rotavirus diversity and evolution. Virus Evol. 6, vez059.

Ito, H., Sugiyama, M., Masubuchi, K., Mori, Y., Minamoto, N., 2001. Complete nucleotide sequence of a group A avian rotavirus genome and a comparison with its counterparts of mammalian rotaviruses. Virus Res. 75, 123–138.

Jayaram, H., Estes, M.K., Prasad, B.V., 2004. Emerging themes in rotavirus cell entry, genome organization, transcription and replication. Virus Res. 101, 67–81.

Johne, R., Reetz, J., Kaufer, B.B., Trojnar, E., 2016. Generation of an avian-mammalian rotavirus reassortant by using a helper virus-dependent reverse genetics system. J. Virol. 90, 1439–1443.

Johne, R., Tausch, S.H., Schilling-Loeffler, K., Ulrich, R.G., 2023. Genome sequence analysis of a novel rotavirus strain indicates a broad genetic diversity of rotavirus A in shrews. Infect. Genet. Evol. 107, 105392.

Katoh, K., Misawa, K., Kuma, K.-I., Miyata, T., 2002. MAFFT: a novel method for rapid multiple sequence alignment based on fast Fourier transform. Nucleic Acids Res. 30, 3059–3066.

Kool, D.A., Matsui, S.M., Greenberg, H.B., Holmes, I.H., 1992. Isolation and characterization of a novel reassortant between avian Ty-1 and simian RRV rotaviruses. J. Virol. 66, 6836–6839.

Kumar, S., Stecher, G., Li, M., Tamura, K., 2018. MEGA X: molecular evolutionary genetics analysis across computing platforms. Mol. Biol. Evol. 35, 1547–1549.

Le, S.Q., Gascuel, O., 2008. An improved general amino acid replacement matrix. Mol. Biol. Evol. 25, 1307–1320.

Li, W., Manktelow, E., von Kirchbach, J.C., Gog, J.R., Desselberger, U., Lever, A.M., 2010. Genomic analysis of codon, sequence and structural conservation with selective biochemical-structure mapping reveals highly conserved and dynamic structures in rotavirus RNAs with potential cis-acting function. Nucleic Acids Res. 38, 7718–7735.

Li, Y., Xia, Z., Peng, J., Zhou, T., Fan, Z., 2013. Evidence of recombination and genetic diversity in southern rice black-streaked dwarf virus. Arch. Virol. 158, 2147–2151.

Martin, D.P., Murrell, B., Golden, M., Khoosal, A., Muhire, B., 2015. RDP4: detection and analysis of recombination patterns in virus genomes. Virus Evol. 1, vev003.

Matthijnssens, J., Ciarlet, M., Rahman, M., Attoui, H., Banyai, K., Estes, M.K., Gentsch, J. R., Iturriza-Gomara, M., Kirkwood, C.D., Martella, V., Mertens, P.P.C., Nakagomi, O., Patton, J.T., Ruggeri, F.M., Saif, L.J., Santos, N., Steyer, A., Taniguchi, K., Desselberger, U., Van Ranst, M., 2008. Recommendations for the classification of group A rotaviruses using all 11 genomic RNA segments. Arch. Virol. 153, 1621–1629.

Matthijnssens, J., Ciarlet, M., McDonald, S.M., Attoui, H., Banyai, K., Brister, J.R., Buesa, J., Esona, M.D., Estes, M.K., Gentsch, J.R., Iturriza-Gómara, M., Johne, R., Kirkwood, C.D., Martella, V., Mertens, P.P.C., Nakagomi, O., Parreno, V., Rahman, M., Ruggeri, F.M., Saif, L.J., Santos, N., Steyer, A., Taniguchi, K., Patton, J. T., Desselberger, U., Van Ranst, M., 2011. Uniformity of rotavirus strain nomenclature proposed by the rotavirus classification working group (RCWG). Arch. Virol. 156, 1397–1413.

McDonald, S.M., Patton, J.T., 2011. Assortment and packaging of the segmented rotavirus genome. Trends Microbiol. 19, 136–144.

Mitake, H., Ito, N., Okadera, K., Okada, K., Nakagawa, K., Tanaka, T., Katsuragi, K., Kasahara, K., Nihongi, T., Tsunemitsu, H., Sugiyama, M., 2015. Detection of avian-like rotavirus A VP4 from a calf in Japan. J. Vet. Med. Sci. 77, 221–224.

Mitchell, D.B., Both, G.W., 1990. Completion of the genome sequence of the simian rotavirus SA11: nucleotide sequences of segments 1, 2, and 3. Virology 177, 324–331.

Nakagomi, O., Nakagomi, T., 2002. Genomic relationships among rotaviruses recovered from various animal species as revealed by RNA–RNA hybridization assays. Res. Vet. Sci. 73, 207–214.

Nei, M., Kumar, S., 2000. Molecular Evolution and Phylogenetics. Oxford University Press, Oxford, New York.

Ngoveni, H.G., van Schalkwyk, A., Koekemoer, J.J.O., 2019. Evidence of intragenic recombination in African horse sickness virus. Viruses 11, 654.

Oki, H., Masuda, T., Hayashi-Miyamoto, M., Kawai, M., Ito, M., Madarame, H., Fukase, Y., Takemae, H., Sakaguchi, S., Furuya, T., Mizutani, T., Oba, M., Nagai, M., 2022. Genomic diversity and intragenic recombination of species C rotaviruses. J. Gen. Virol. 103, 001703.

Oshima, K., Setaka, R., Inui, H., Kobayashi, Y., Suzuki, Y., 2022. Co-evolving pairs of complementary nucleotide sequence regions containing compensatory divergences and polymorphisms in rotavirus genomes. Gene Rep. 29, 101709.

Patzina-Mehling, C., Falkenhagen, A., Trojnar, E., Gadicherla, A.K., Johne, R., 2020. Potential of avian and mammalian species A rotaviruses to reassort as explored by plasmid only-based reverse genetics. Virus Res. 286, 198027.

Rambaut, A., 2018. FigTree. http://tree.bio.ed.ac.uk/software/figtree.

Rotavirus Classification Working Group: RCWG, 2021. List of accepted genotypes. https://rega.kuleuven.be/cev/viralmetagenomics/virus-classification/rcwg.

Schnepf, N., Deback, C., Dehee, A., Gault, E., Parez, N., Garbarg-Chenon, A., 2008. Rearrangements of rotavirus genomic segment 11 are generated during acute infection of immunocompetent children and do not occur at random. J. Virol. 82, 3689–3696.

Settembre, E.C., Chen, J.Z., Dormitzer, P.R., Grigorieff, N., Harrison, S.C., 2011. Atomic model of an infectious rotavirus particle. EMBO J. 30, 408–416.

Suzuki, Y., Gojobori, T., Nakagomi, O., 1998. Intragenic recombinations in rotaviruses. FEBS Lett. 427, 183–187.

Suzuki, Y., Yaeshiro, M., Uehara, D., Ishihara, R., 2024. Shared clusters between phylogenetic trees for genomic segments of *Rotavirus A* with distinct genotype constellations. Gene Rep. 36, 101956.

Trask, S.D., McDonald, S.M., Patton, J.T., 2012. Structural insights into the coupling of virion assembly and rotavirus replication. Nat. Rev. Microbiol. 10, 165–177.

Trojnar, E., Otto, P., Johne, R., 2009. The first complete genome sequence of a chicken group A rotavirus indicates independent evolution of mammalian and avian strains. Virology 386, 325–333.

Trojnar, E., Sachsenroder, J., Twardziok, S., Reetz, J., Otto, P.H., Johne, R., 2013. Identification of an avian group A rotavirus containing a novel VP4 gene with a close relationship to those of mammalian rotaviruses. J. Gen. Virol. 94, 136–142.

Troupin, C., Schnuriger, A., Duponchel, S., Deback, C., Schnepf, N., Dehee, A., Garbarg-Chenon, A., 2011. Rotavirus rearranged genomic RNA segments are preferentially packaged into viruses despite not conferring selective growth advantage to viruses. PloS One 6, e20080.

Valusenko-Mehrkens, R., Gadicherla, A.K., Johne, R., Falkenhagen, A., 2023. Strain-specific interactions between the viral capsid proteins VP4, VP7 and VP6 influence rescue of rotavirus reassortants by reverse genetics. Int. J. Mol. Sci. 24, 5670.

Woods, R.J., 2015. Intrasegmental recombination does not contribute to the long-term evolution of group A rotavirus. Infect. Genet. Evol. 32, 354–360.
Xu, S., Ahmed, L.U., Stuckert, M.R., McGinnis, K.R., Liu, Y., Tan, M., Huang, P., Zhong, W., Dandan Zhao, D., Jiang, X., Kennedy, M.A., 2020. Molecular basis of P [II] major human rotavirus VP8* domain recognition of histo-blood group antigens. PLoS Pathog. 16, e1008386.
Yin, X., Zheng, F.-Q., Tang, W., Zhu, Q.-Q., Li, X.-D., Zhang, G.-M., Liu, H.-T., Liu, B.-S., 2013. Genetic structure of rice black-streaked dwarf virus populations in China. Arch. Virol. 158, 2505–2515.
Yoshida, R., Nei, M., 2016. Efficiencies of the NJp, maximum likelihood, and Bayesian methods of phylogenetic construction for compositional and noncompositional genes. Mol. Biol. Evol. 33, 1618–1624.
Zhang, Z., Li, N., Hou, C., Gao, K., Tang, X., Guo, X., 2020. Analysis of reassortant and intragenic recombination in cypovirus. Virol. J. 17, 48.